2021-09

Extreme responses of a hinged raft type wave energy convertor

Tosdevin, Tom

Extreme responses of a hinged raft type wave energy convertor

Tom Tosdevin, Siya Jin, Andrea Caio, Dave Simmonds, Martyn Hann and Deborah Greaves

Abstract—**Much attention has been paid in recent years to the determination of design loads for moored floating structures and the application of established methodologies for fixed structures have been found to be ineffective. This paper experimentally investigates extreme responses of a lazy S moored 1:20 scale model of Mocean Energy's Blue Star wave energy convertor (WEC) along the 1 year return contour. The device is a hinged raft type WEC and the extreme responses studied include mooring loads and snatch load events. Long irregular wave time series are used in the estimation of extreme value distributions of the mooring load for particular sea states. Conditional random response wave and constrained new wave profiles are used to study and support the predictions. Wave calibration and the impact of wave breaking on the physical realisation of response conditioned focus waves and extreme value distribution (EVD) predictions are discussed.**

Index Terms—**WEC, Hinged Raft, Extreme Responses, Reliability, Moorings.**

I. Introduction

THE ability of floating offshore renewable energy (ORE) devices, such as wave energy converters (WECs) to survive extreme sea conditions has been identified as an important area for design improvements. The accurate prediction of the extreme loads on a device is essential for reliability analysis and reducing the levelised cost of energy (LCOE). This is an area that has been studied extensively in ship design and so methods developed in that field are potentially very useful and have been applied in this work. In the design process, loads with a specific probability of occurrence which a device should be designed to withstand need predicting, these are termed design loads. They are often predicted using a contour method where a design sea is identified and a particular percentile of the extreme value distribution (EVD) of the response of interest read off. Predicting the EVD, the distribution of the single largest value in a 3hour exposure time, of a response of a floating ORE device is found to be more difficult than for fixed devices. The EVD of the response in a specific sea state is sometimes referred to as the short-term extreme response distribution (SERD). The EVD predictions are typically made from long irregular wave time series and are likely to require more data the more dynamic a case is.

Focus and constrained focus wave methods are examples of short design waves which have been applied as a way of studying generic extreme responses e.g. [1] or in the hope that they can be used to reduce the amount of time required in the prediction of design loads. They may be able to speed up the identification of design loads if they can predict the EVD with a shorter simulation time than that required using long irregular waves with methods utilising large numbers of constrained focus waves such as those developed in [2], [3] or by studying the possibility of relating a single run to a particular percentile response representing a design load e.g. [4]. The validity of response conditioned focus wave methods is dependent on the condition that the device responses are small perturbations from those predicted by linear theory [5]. It is recognised in ship design that it is not practical to predict the EVD of a response using constrained focus waves in physical tests because hundreds, if not thousands, of runs would be required [6]. It is unlikely then to be possible at all for the more dynamic examples of floating ORE, judging by the large variance in responses produced by identical focus waves constrained into different irregular backgrounds reported on in [1]. For these reasons no attempt is made in this work to predict the design load or the EVD using constrained focus wave methods as done in [2], [3]. However, constrained focus waves may still provide useful data on how a device responds to extreme loads, provide inputs to structural models and lend limited support to the EVDs predicted from long irregular wave time series. This paper explores the ability of different constrained focus wave methods to produce extreme responses at the high percentiles of the EVD of the design sea state. For constrained focus waves to be of practical use during physical scale model testing they must be produced reasonably quickly and accurately. The main aim of this paper is to investigate how constrained focus waves may be used in physical scale model testing to reproduce extreme loads predicted by the EVDs. A discussion of the complicating effects of snatch loading, wave calibration and wave breaking is therefore undertaken in an attempt to provide useful information to those considering the use of constrained

ID:2128, Wave hydrodynamic modelling. This work was supported by the Engineering and Physical Sciences Research Council (EPSRC, reference EP/S000747/1) through the Supergen ORE hub. ...

Tom Tosdevin is a PhD student with the School of Engineering Computing and Mathematics at the University of Plymouth. University of Plymouth, Plymouth, Devon PL4 8AA, UK (e-mail:Tom.Tosdevin@postgrad.Plymouth.ac.uk).

Siya Jin is an ORE research fellow at the University of Plymouth. (e-mail: Siya.Jin@Plymouth.ac.uk).

Andrea Caio is an EngD candidate at the Industrial Doctorate Centre on Offshore Renewable Energy (IDORE), researching in collaboration with Mocean Energy, and based at the School of Engineering, The University of Edinburgh, Sanderson Building, Robert Stevenson Road, Edinburgh, EH9 3FB, U.K. (e-mail: andrea.caio@ed.ac.uk).

Dave Simmonds is an associate professor in coastal engineering at the University of Plymouth. (e-mail: D.Simmonds@Plymouth.ac.uk).

Martyn Hann is a lecture in coastal engineering at the University of Plymouth. (e-mail: Martyn.Hann@Plymouth.ac.uk).

Deborah Greaves is a professor of offshore engineering at the University of Plymouth. (e-mail: Deborah.Greaves@Plymouth.ac.uk).

Fig. 1. Subsurface view of model WEC and Lazy S mooring line - experimental setup

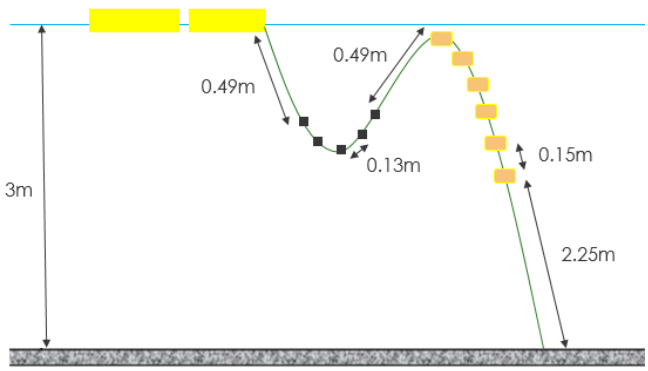

Fig. 2. Sketch of the Lazy S mooring (not drawn to scale), distances between masses and floats are constant and given from centre to centre of each mass/float

focus waves in future.

II. Device description

A 1:20 scale model of Mocean Energy's Blue Star WEC was used to study extreme mooring loads. This is a 2 body hinged raft type WEC which was moored using a 'Lazy S' arrangement (Fig. 1) at a water depth of 3m. The model did not contain any power take off (PTO) in line with the envisaged survival strategy that involves switching off the PTO (i.e. free hinge). The Lazy S mooring consisted of 6 evenly spaced $1.6 \times 10^{-5} m^3$ floats and 5 evenly spaced 3.8g masses with a line length between fairlead and tank bottom of 4.5m. The line had a high axial stiffness and a bending stiffness of $1.3 \times 10^{-3} N/m^2$. See Fig.2 for mooring details. The device responses selected for study were the mooring load and maximum relative pitch angles (hogging and sagging). Only the mooring load responses measured using a load cell at the fairlead position are presented in this paper with their magnitudes obscured for commercial confidentiality. Further details of a previous iteration of the device can be found in [7].

III. Contour method

The contour method for predicting the design load of a response involves searching the 1 in x year return contour in Hs Tp space and identifying the sea state for which the y percentile of the EVD gives the largest response. This sea state is then defined as the design sea state and the response at the y percentile the design load. The percentile, y, would be taken as the median (50th percentile) if the variation of the response were to be neglected. However, as this variation is considered important in offshore engineering a larger percentile is selected. It is often estimated based on empirical observations from the offshore engineering industry according to the return period x [8]. The EVD is defined here as the distribution of the 1 in 3 hour largest values and is determined from a peak over threshold (POT) method, where the peaks data is gathered using long irregular wave time series. All irregular waves in this study were generated using a JONSWAP spectrum with gamma equal to one. The statistical uncertainty in the EVD predictions reduce with the increased quantity of peaks data collected; [9] recommends a minimum of 18 hours (full scale equivalent) but this amount of data is rarely collected due to time constraints. The default threshold used in this study is taken as the mean plus 1.4 times the standard deviation following [10]. This contour process is recommended in various design standards for use in physical model testing e.g. [11], [12]. The contour method will be utilised in this work as other more accurate long-term methods require too much data to be collected to make them suitable for use in physical modelling.

IV. Constrained focus waves

Focus wave approaches seek to bypass the extensive simulations required to study extremes when running long irregular wave time series by only simulating the single wave profile that leads to the extreme response. The NewWave approach developed by Tromans et al. [13] treats the generation of a sea state profile as a Gaussian process and uses the spectral density to generate the average profile of the extreme wave by scaling the different frequency components according to their energy contributions. The NewWave method has been used extensively in the ORE WEC literature and the governing equations described [14], [15], [16], [17], and so they are not outlined here. More recently response conditioned focus waves, such as the most likely extreme response (MLER) method [18], have been applied using CFD simulations [19], [20], [21], [22]. The MLER wave is a response conditioned focus wave which uses the magnitude and phase of the linear RAO to estimate the average wave profile leading to extremes for the response of interest. However, for many types of floating ORE solitary focus waves are found not to produce responses as large as those from other methods [1], [20], [22]. This is largely due to history effects not being considered which are particularly important for the mooring loads when there is a slow surge drift. For this reason methods to constrain the focus waves into random irregular wave backgrounds

have been used in this study. Goteman et al. [23] constrained NewWaves into regular wave backgrounds and Hann et al. [1] constrained NewWaves into random irregular backgrounds to study how the extreme mooring loads of taught moored, bottom referenced point absorber WECs are influenced by the background waves. The natural progression would be to study the effect of constraining response conditioned focus waves into random irregular backgrounds which is the focus of this work. The conditional random response wave (CRRW) method developed in Dietz [3], the result of which is a MLER profile constrained into a short random irregular background, was applied in this study.

The MLER and CRRW methods as set out in [3], [6] are outlined below.

The surface elevation time series can be given as

$$\zeta(t) = \sum_{n=1}^{N} a_{\zeta;n}[V_n \cos(-\omega_n t) + W_n \sin(-\omega_n t)] \quad (1)$$

Where N is the number of wave components, V_n and W_n are independent standard normal random variables and $a_{\zeta;n}$ is the spectral amplitude. The method follows a Slepian model process where the conditioned values of V_n and W_n used to constrain the desired response conditioned focus wave are $V_{n;c}$ and $W_{n;c}$

$$\begin{aligned} V_{n;c} = V_n &- \frac{a_{M;n}}{m_2 m_0 - m_1^2}(m_2 - \omega_n m_1) S_1 \cos(\theta_{M;n}) \\ &- M_c(m_2 - \omega_n m_1)\cos(\theta_{M;n}) \\ &+ (\omega_n m_0 - m_1) S_2 \sin(\theta_{M;n}) \\ &+ (\omega_n m_1 - m_2) S_3 \sin(\theta_{M;n}) \\ &+ (\omega_n m_0 - m_1) S_4 \cos(\theta_{M;n}) \\ &- M_c \omega_M (\omega_n m_0 - m_1)\cos(\theta_{M;n}) \end{aligned} \quad (2)$$

$$\begin{aligned} W_{n;c} = W_n &- \frac{a_{M;n}}{m_2 m_0 - m_1^2}[(m_2 - \omega_n m_1) S_1 \sin(\theta_{M;n}) \\ &- M_c(m_2 - \omega_n m_1)\sin(\theta_{M;n}) \\ &- (\omega_n m_0 - m_1) S_2 \cos(\theta_{M;n}) \\ &- (\omega_n m_1 - m_2) S_3 \cos(\theta_{M;n}) \\ &+ (\omega_n m_0 - m_1) S_4 \sin(\theta_{M;n}) \\ &- M_c \omega_M (\omega_n m_0 - m_1)\sin(\theta_{M;n})] \end{aligned} \quad (3)$$

$$S_1 = \sum_{n=1}^{N} a_{M;n}[V_n cos(\theta_{M;n}) + W_n sin(\theta_{M;n})] \quad (4)$$

$$S_2 = \sum_{n=1}^{N} a_{M;n}\omega_n[V_n sin(\theta_{M;n}) - W_n cos(\theta_{M;n})] \quad (5)$$

$$S_3 = \sum_{n=1}^{N} a_{M;n}[-V_n sin(\theta_{M;n}) + W_n cos(\theta_{M;n})] \quad (6)$$

$$S_4 = \sum_{n=1}^{N} a^e_{M;n}\omega_{e;n}[V_n cos(\theta^e_{M;n}) + W_n sin(\theta^e_{M;n})] \quad (7)$$

Where $a_{M;n}$ is the spectral amplitude of the response spectrum, M_c is the target response amplitude and $\omega_M = \frac{m_1}{m_0}$. The conditioned values $V_{n;c}$ and $W_{n;c}$ are then substituted in place of V_n and W_n in (1) to produce the embedded wave time series. The solitary MLER wave is obtained by defining V_n and W_n as Gaussian random variables with zero mean and standard deviation equal to $a_{M;n}$ rather than one.

Typically a Rayleigh distribution is assumed for the peaks and the focus wave amplitudes are scaled to the most likely value of the EVD, this being the peak of the distribution (the mode). For a Rayleigh distribution this is roughly the 38th percentile [24] and is estimated using

$$A = \sqrt{2m_0 ln(n)} \quad (8)$$

Where n is the expected number of peaks in the 3 hour exposure time which is often assumed to be 1000. To determine a more accurate amplitude to scale to, the number of peaks and Rayleigh distribution are defined below from the spectral moments;

An approximation of the expected number of peaks for a non-narrow-banded spectrum, defined as $\epsilon < 0.9$, is

$$n = \frac{1}{4\pi}\left(\frac{1+\sqrt{1-\epsilon^2}}{\sqrt{1-\epsilon^2}}\right)\sqrt{\frac{m_2}{m_0}} \quad (9)$$

Where ϵ is the bandwidth parameter defined as

$$\epsilon = \frac{\sqrt{1-m_2^2}}{m_0 m_4} \quad (10)$$

Where the spectral moments m_k are

$$m_k = \int_0^k \omega^k S_r(\omega) d\omega \quad (11)$$

The EVDs of the wave and response amplitudes were predicted assuming a Rayleigh distribution for the peaks, the EVD is given by;

$$f_{\tilde{X}_n}(x) = n\left(\frac{x}{\sigma^2}e^{-\frac{x^2}{2\sigma^2}}\right)\left(1 - e^{-\frac{x^2}{2\sigma^2}}\right)^{n-1} \quad (12)$$

The CRRW and CNW profiles in this work were scaled to the 99th percentile of the EVDs of the response peaks and wave amplitude peaks, by substituting in the sea spectrum $S(\omega)$ in place of the response spectrum for the CNWs in (11), respectively. For offshore engineering, in the absence of a response model, the design load is commonly taken above the 70th percentile [25]. However, to produce responses at these high percentiles the wave and response amplitudes are here scaled to the 99th percentile for several reasons;

- History effects are important but unaccounted for and by using a higher percentile the profiles are more likely to produce responses at the higher percentiles.
- The distributions of the extreme wave and response amplitudes are based on linear theory and so likely to be under predictions due to neglecting the nonlinear evolution of waves. The Rayleigh distribution is found to under predict extremes from field measurements [26].

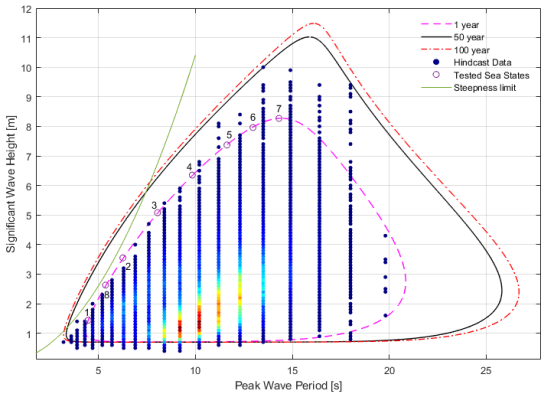

Fig. 3. EMEC full scale site data, numbered sea states correspond to those in table 1

- There are discrepancies between the target and physically realised wave amplitudes (experimental error) and so a range of values around the target will be generated in practice.

V. Test Site and Wave Climate

The environmental characterisation was performed on the EMEC site off Scotland using 30 years of hindcast data. The estimation of the environmental contour is based on the Inverse First Order Method (IFORM), together with a Weibull distribution for Hs and conditional log-normal distribution for $Tp|Hs$ [27]. The significant steepness is defined as $S_p = \frac{2\pi H_s}{gT_p^2}$ and the limiting steepness taken as $S_p \leq \frac{1}{15}$ [11], [28]. The limiting steepness defines the curve in Fig.3 to the left of which wave breaking renders the sea states unphysical. The closer a sea state is to this limit the more difficult it is to physically reproduce the target surface elevations of the constrained focus wave runs due to an increased frequency of wave breaking as the target focus waves may be unphysical. The increased steepness also leads to greater deviations from linear wave theory. 8 sea states along the contour were studied.

VI. Wave Calibration

It is important to assess the accuracy of the physical realisation of the constrained focus waves and apply some form of calibration. There does not seem to be much on calibrating exact surface elevation time series in the ORE literature as it is more often capturing the statistics of the sea spectrum during long irregular waves which is of interest. Where it has been tried a frequency domain correction is usually applied using a phase amplitude iteration scheme such as in [29]. This is potentially very time consuming if a large number of iterations is required. Preliminary tests suggested that a single phase correction resulted in a large improvement in the accuracy of the generated solitary focus wave profile. The solitary NW and MLER profiles were therefore calibrated in this way by taking a fast Fourier transform (FFT) of the target and measured surface elevations and adding the phase difference to the input signal.

Two types of calibration were compared for CRRWs scaled to the 80th percentile response of the Rayleigh EVD in SS4 ($Hs = 0.318m$, $Tp = 2.2s$). The first method tried, termed the individual calibration, was based on a section of the surface elevation defined as the time step of the focus wave, 52s, plus/minus 4s. This small portion of the time series was selected for calibration as it contains the embedded focus wave, the rest of the time series is random and so it's accurate reproduction is less important. An FFT was then performed on this section of the measured wave and compared to the FFT of the corresponding section of the target wave. The phase difference was then added to the input signal and the wave rerun; this process needed repeating for every individual CRRW and so increases the lab time required relative to no calibration by a factor of more than 2. The second method applied the phase correction from the solitary MLER to the CRRW runs and so did not increase the lab time needed, this is termed the solitary focus wave calibration.

An important source of error affecting the device response is the error between the target and physically generated wave surface elevation. Not only is accuracy important but so too is the amount of time required for the calibration. There does not appear to be a standard way of assessing the accuracy of the generated wave profiles. In this study it is the accuracy of the focus wave constrained at 52 seconds which is of most importance as the background is random. To assess the improvement in the accuracy due to the calibration method the surface elevation is analysed from 52-T_t to 52s where T_t is the time step of the trough preceding the focus time (52s). The mean square error (MSE) of the uncalibrated and calibrated waves are then calculated and the profiles shifted in time by up to 1.5s so that the values are minimised. This time shift was appropriate as the exact time that the focus wave occurs was not important within a few seconds. The Brier skill score [30] is then calculated to determine whether the calibration has produced an improvement on the uncalibrated wave. A positive value means the calibration was a better fit to the target with a value of 1 being an exact fit. A negative value means the uncalibrated wave was a better fit.

$$BSS = 1 - \frac{MSE(Y,X)}{MSE(B,X)} \tag{13}$$

Here the baseline prediction is taken as the uncalibrated surface elevation so $MSE(Y,X)$ is the mean square error of the calibration to the target and $MSE(B,X)$ the mean square error of the uncalibrated wave relative to the target.

VII. Results and Discussion

A. Searching the contour

The full scale equivalent of a minimum of 3 hours of irregular waves were run for sea states 2-7 shown in table 1. SS5 was identified as the one most likely to be the design state for the mooring load and 18 hours of data (full scale equivalent) collected in line with [9].

TABLE I
SURGE OFFSET BY SEA STATE AT MODEL SCALE

Sea state	Hs	Tp	Mean surge position
1	0.072m	1s	1.15m
2	0.178m	1.4s	1.49m
3	0.254m	1.8s	1.41m
4	0.318m	2.2s	1.34m
5	0.369m	2.6s	1.32m
6	0.398m	2.9s	0.89m
7	0.413m	3.2s	0.65m
8	0.132m	1.2s	1.38m

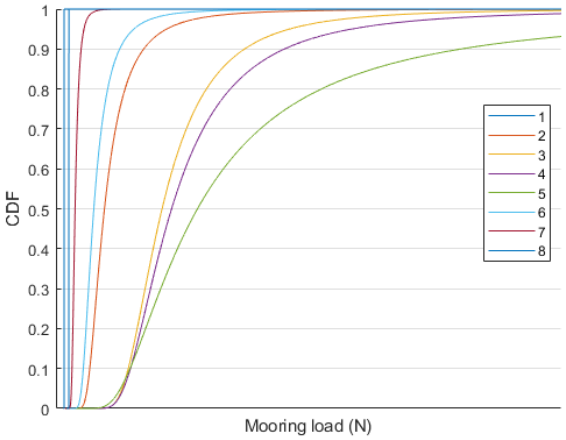

Fig. 4. EVD force at fairlead. The full scale equivalent of 18 hours of irregular wave data was used in the estimation of the EVD of SS4 and SS5, 3 hours for SS2, SS3, SS6 and SS7 and 1 hour for SS1 and SS8.

Fig.4 gives the EVD predictions using all the irregular wave data. Fig.4 can be understood in the context of Table 1, SS5 produces the largest responses due to the combination of large surge drift position and Hs. The average surge position significantly reduces for SS6 and SS7. The EVD predictions for SS3-5 were larger due to the presence of snatch loads which occurred when the mooring line became taught, leading to much higher loads.

B. Impact of preceding wave

By identifying a wave profile resulting in a snatch load event and varying the amount of preceding wave time series generated the importance of the history effects and the surge drift position in particular can be demonstrated, see Fig. 5. As the amount of preceding wave generated is increased so too does the surge drift position, there is not a significant increase after around 35 seconds in the example shown. Here the surge position is given according to the position of the hinge connecting the rafts. To allow for the surge drift to establish all the focus waves were constrained at 52s and each run lasted 57s. The drift has a significant effect on the mooring loads and is a second order effect, it illustrates why solitary focus waves do not produce extremes, why any estimate of an EVD based on the linear RAOs will be inaccurate and why the same focus

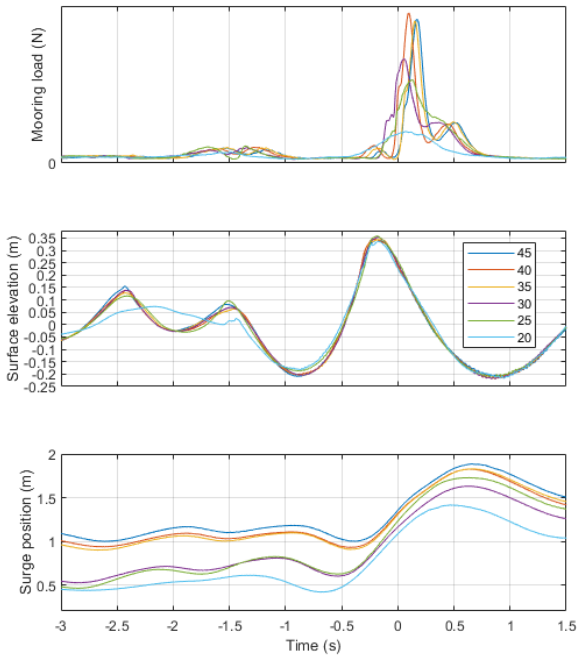

Fig. 5. Effect of varying the length of the irregular wave background on the mooring load, the amount of preceding wave in seconds is given by the legend. The first 7 seconds of each run consists of paddle inactivity and ramp time. The surface elevation is given from a wave gauge located at 1.47m from the zero surge position. The surge position given is that at the hinge.

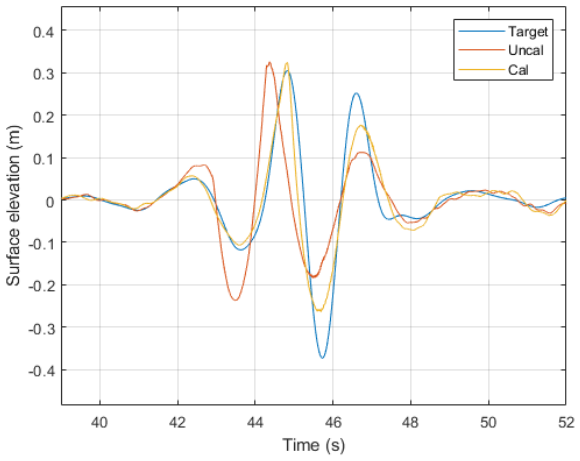

Fig. 6. Solitary MLER wave calibration SS5, scaled to the 99th percentile of the linear response EVD. The calibration method applied was for the solitary focus wave outlined at the beginning of section VI.

wave embedded in different backgrounds will produce a wide range of mooring loads making it impractical to predict design loads using constrained focus waves for dynamic floating ORE.

C. Wave calibration

Fig. 6 shows that to produce accurately the profiles with large amplitudes it is necessary to perform some form of calibration. In the cases considered here the extreme response occurs at 45 seconds so it is the

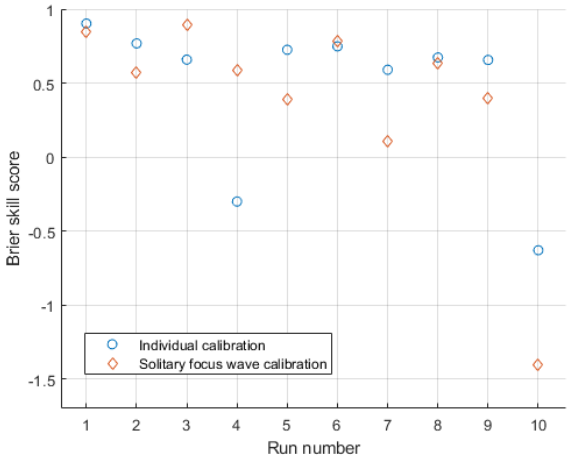

Fig. 7. Brier skill score calibration comparison, 80th percentile CRRW profiles for SS4.

accurate reproduction of the profile up to 45s which is of primary concern.

It can be seen in Fig.7 that the calibration produced an improvement (A BSS above 0) in 8/10 cases for the individual calibration runs and 9/10 for the solitary focus wave calibration runs. The instances where the calibration was not an improvement were due to wave breaking. There was no significant difference in the improvement using the individual compared to the solitary focus wave calibration but there was a substantial difference in the time requirement. Therefore the solitary focus wave calibration method was used for the constrained focus wave profiles.

D. Constrained focus waves

20 CRRW (black line Fig.8a) were first run for SS5 but it was apparent that the profile did not match the average profile (red line Fig.8a and 8b) which led to the extreme mooring loads from the long irregular wave time series as can be seen in Fig.8a. The 18 hours of irregular waves were split into six 3 hour runs and the empirical profile was calculated from the average of the profiles which resulted in the largest mooring load from each of the six runs. 30 CNWs (black line Fig.8b) were then run as they were found to more closely resemble the empirical average profile Fig.8b, a phase shifted CNW which was a better fit was also tried but is not shown here as the loads generated were not significantly different to those of the CNW. The mooring loads generated by the CRRW, CNW and empirical runs are compared to the EVD predicted from the long irregular waves in Fig.9. It can be seen that the CNWs produced a small number of extremes at the higher end of the EVD. The effects of wave amplitude on the mooring load generated are demonstrated in Fig.10, the range of CNW amplitudes about the 99th percentile target of 0.443m can also be seen. There is no shared target surface elevation amplitude for the CRRWs to compare with as the response peak occurs after the surface elevation peak. The CRRWs failed to produce extremes as large as the CNWs due to the abrupt change in system behaviour brought on

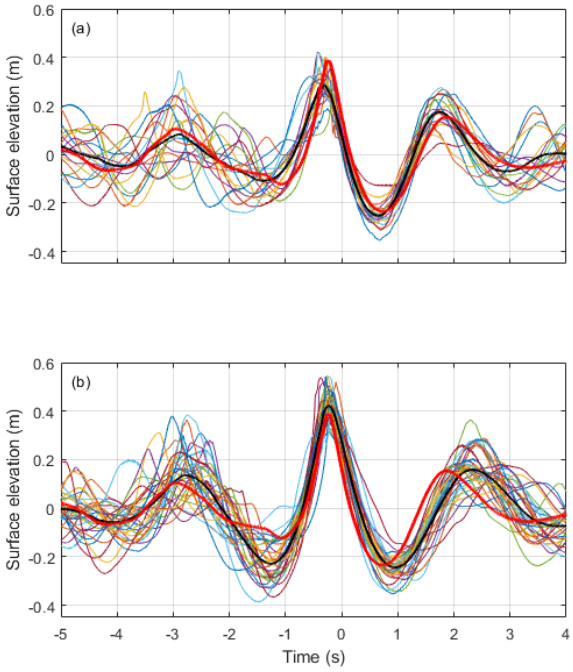

Fig. 8. (a) 20 CRRW profiles with black giving the average and red the average for the 6 empirical extremes from the 18hrs of irregular waves. (b) 30 CNW profiles with black giving the average and red the average for the 6 empirical extremes from the 18hrs of irregular waves.

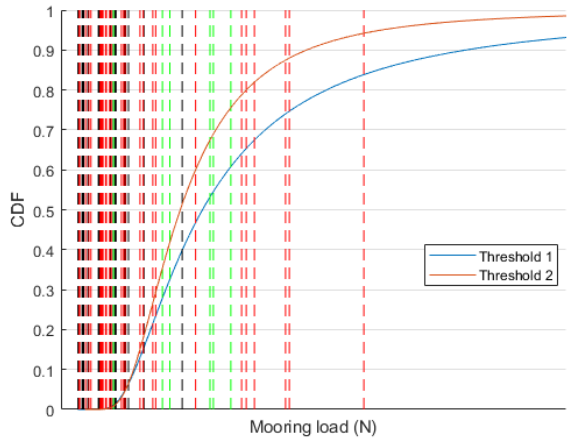

Fig. 9. CRRW, CNW, EVD comparison. CNW responses are given by red dashed vertical lines, CRRWs black and the 6 empirical 1 in 3hr extremes from the long irregular waves are green. The EVD CDF for threshold 1 is given in blue, threshold 2 is given by the solid red curve. Threshold 2 uses a larger threshold. Force magnitudes have been obscured by removing the x axis values.

by the snatch loads. The CRRWs are based on linear RAOs and so because the system behaviour departs from those RAOs, the CRRWs no longer produce the extremes. This result serves as a reminder that response conditioned methods are only as valid as the linear RAOs they are calculated from.

The constrained new waves produced some higher percentile responses on the predicted EVD. However, considering the wave amplitudes were scaled to the 99th percentile of the predicted extreme wave ampli-

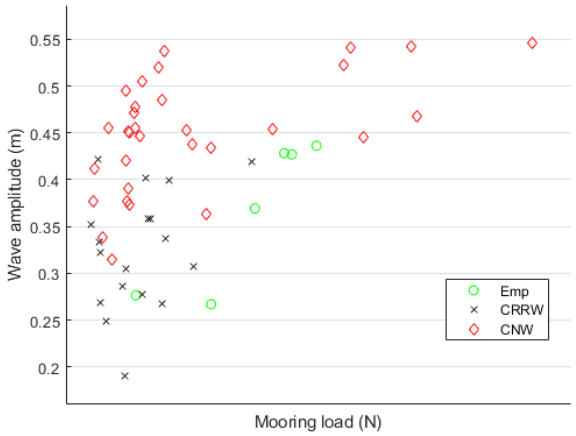

Fig. 10. Largest mooring load vs largest wave amplitude for the 20 CRRWs and 30 CNWs occurring approximately at the selected time step of the extreme (52s) and the empirical profiles producing the largest responses for SS5.

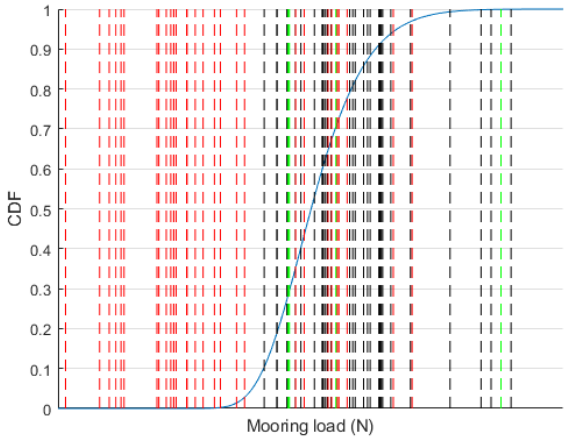

Fig. 11. CRRW CNW EVD comparison. CRRWs are black, CNWs red and the 4 empirical 1 in 3hr extremes from the long irregular waves are green. The EVD CDF is calculated based on the full scale equivalent of 12 hours of irregular waves. The x axis is obscured.

tude distribution, few higher percentile values were observed. This is likely due to the difficulty in producing snatch loads as they are dependent on chaotic history effects, but also because the snatch loading complicates the prediction of the EVD as they likely change the shape of the distribution above a threshold. The EVD prediction for the sea state containing snatch loads therefore would be improved by determining the threshold to fit the distribution by the definition of the snatch loads, as is done in [31]. Defining the snatch load cases however is not straightforward. A classification using the separation distance of the fairlead and anchor positions was attempted but it was found that this distance being at a maximum was no guarantee of a large mooring load. The definition of the threshold then becomes somewhat arbitrary. Threshold 1 in Fig.9 is based on the mean and standard deviation, the same as that used to compare the sea states in Fig.4. Threshold 2 is taken at a larger mooring load chosen to define the snatch loads as a high value which occurs when the separation distance of anchor and fairlead is at a maximum. Threshold 1 corresponds to the 96.7th percentile of the data and so the EVD is calculated from 271 peaks, threshold 2 to the 98.6th percentile using 106 peaks. Threshold 2 therefore uses much less data in the prediction of the EVD. The problem of threshold selection is present even in the absence of a change in system behaviour and it would seem prudent to impose a mooring design criteria that precludes the possibility of snatch loading to the greatest extent possible as they result in significantly increased mooring loads. For these reasons the accuracy of the EVD is not considered further here. To remove the complicating effects of snatch loading a less extreme sea state with the same Tp as SS5 but a much smaller Hs is studied for comparison.

E. Smaller sea state

The full scale equivalent of 12 hours of irregular waves and 30 CNW and 30 CRRW profiles were run

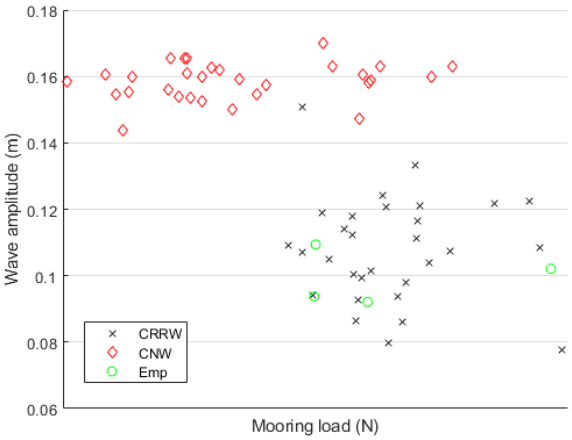

Fig. 12. Largest mooring load vs largest wave amplitude for the 30 CRRWs and 30 CNWs occurring approximately at the selected time step of the extreme (52s) and the empirical profiles producing the largest responses for SS9.

for a smaller sea state with $Tp = 2.6s, Hs = 0.1252m$ which will be referred to as SS9. The EVD was calculated based on the POT method using the threshold calculated from the mean and standard deviation. Fig.11 and Fig.12 demonstrate that the 30 CRRWs produced mooring loads larger than the 30 CNWs and at the upper percentiles of the EVD. The target CNW amplitude was 0.151m. It can be seen from Fig.12 that even in the absence of snatch loads CNWs with virtually identical amplitudes produce a wide range of mooring loads due to the importance of history effects.

F. Wave breaking

It is worth mentioning that wave breaking in sea states close to the steepness limit result in significant problems for physical testing. The proximity of SS1, SS8 and SS2 in particular, to the steepness limit made it impossible to produce accurately any surface elevation profiles for constrained focus waves in these sea states. The profile of the wave producing the

extreme response cannot scale up indefinitely due to the occurrence of ever more wave breaking as the amplitude is increased. The impact of wave breaking on the prediction of the EVD is uncertain; there is currently no upper limit and how to impose one is an open question. Being able to accurately determine the point at which a wave becomes unphysical would be useful in attempting to solve these issues.

VIII. Conclusions and future work

The CRRW profiles successfully produced extremes at the higher end of the EVD in sea states where snatch loading did not occur. However, the extreme responses in sea states in which snatch loading did occur were more successfully produced by CNWs. This result serves as a reminder that response conditioned methods are only appropriate when the behaviour of the system is unchanging over the range of possible wave sequences for the sea state. It is a likely constraint on mooring design to minimise the risk of snatch loading and so it is perhaps not worth spending too much time on this problem. On the other hand, other events which may cause abrupt changes in device behaviour exist, snap loads of tension leg or catenary moored platforms or the end stops of a PTO being reached for example, which may make this kind of event worthy of future study. Snatch loads have also been found to produce extreme mooring loads for other existing WEC devices and mooring arrangements [32].

This paper demonstrates how constrained focus waves can be used during physical testing to produce useful data on the extreme responses of ORE devices around the design load. It also shows how they can be used to lend support to EVD predictions in the limited sense that if the constrained focus waves do not produce responses at the higher percentiles of the EVD then it is likely that either the prediction of the EVD or the prediction of the average wave profile leading to the extremes is incorrect. It is, to the best of the authors' knowledge, the first example of using constrained response conditioned focus waves in an ORE context. It is worth reiterating that the EVD has a large associated uncertainty as does the chosen percentile representing the design load and the short wave profiles are not used in the EVD or design load predictions. Therefore spending large amounts of precious lab time on calibration to improve the physical reproduction of the constrained focus waves would seem unwise, particularly as the variation in the response appears to have more to do with chaotic history effects than with the errors in the physical realisation of the target embedded wave profiles. This is demonstrated most clearly by the range in responses produced by similar amplitude CNWs in Fig.10 and Fig.12. 20-30 profiles can be run in an hour using the phase correction calculated from the solitary focus wave calibration. Care should be taken when using response conditioned methods as changes in system behaviour, or wave breaking resulting in the target profiles being unphysical, may render them invalid. The effects of wave breaking on the prediction of the EVDs and physical realisation of constrained focus waves is an important area for future work.

References

[1] M. Hann, D. Greaves, A. Raby, and B. Howey, "Use of constrained focused waves to measure extreme loading of a taut moored floating wave energy converter," *Ocean Engineering*, vol. 148, pp. 33–42, 2018.

[2] P. H. Taylor, P. Jonathan, and L. A. Harland, "Time domain simulation of jack-up dynamics with the extremes of a gaussian process," 1997.

[3] J. S. Dietz, *Application of conditional waves as critical wave episodes for extreme loads on marine structures*. Technical University of Denmark, 2005.

[4] J. Van Rij, Y.-H. Yu, and R. G. Coe, "Design load analysis for wave energy converters," in *International Conference on Offshore Mechanics and Arctic Engineering*, vol. 51319. American Society of Mechanical Engineers, 2018, p. V010T09A031.

[5] D. H. Kim, "Design loads generator: Estimation of extreme environmental loadings for ship and offshore applications." Ph.D. dissertation, 2012.

[6] I. Drummen, M. Wu, and T. Moan, "Numerical and experimental investigations into the application of response conditioned waves for long-term nonlinear analyses," *Marine Structures*, vol. 22, no. 3, pp. 576–593, 2009.

[7] A. Caio, T. Davey, and J. C. McNatt, "Preliminary hydrodynamic assessment of mocean energy's blue star wec via fast-turnaround physical model testing," in *14th European Wave and Tidal Energy Conference; under review*. European Tidal and Wave Energy Conference, 2021.

[8] R. G. Coe, C. Michelen, A. Eckert-Gallup, and C. Sallaberry, "Full long-term design response analysis of a wave energy converter," *Renewable Energy*, vol. 116, pp. 356–366, 2018.

[9] I. E. Commission *et al.*, *Marine Energy: Wave, Tidal and Other Water Current Converters. Tidal Energy Resource Assessment and Characterization*. International Electrotechnical Commission, 2015.

[10] C. Michelen and R. Coe, "Comparison of methods for estimating short-term extreme response of wave energy converters," in *OCEANS 2015-MTS/IEEE Washington*. IEEE, 2015, pp. 1–6.

[11] D. N. V. AS, "Environmental conditions and environmental loads," *Høvik, Norway: DNV GL. Available at: https://rules. dnvgl. com/docs/pdf/DNV/codes/docs/2014-04/RP-C205. pdf. Accessed March*, vol. 15, p. 2018, 2014.

[12] N. NORSOK, "003, 2017," *NORSOK Standard N-003*, 2017.

[13] P. S. Tromans, A. R. Anaturk, P. Hagemeijer *et al.*, "A new model for the kinematics of large ocean waves-application as a design wave," in *The first international offshore and polar engineering conference*. International Society of Offshore and Polar Engineers, 1991.

[14] M. Hann, D. Greaves, and A. Raby, "Snatch loading of a single taut moored floating wave energy converter due to focussed wave groups," *Ocean Engineering*, vol. 96, pp. 258–271, 2015.

[15] P.-H. Musiedlak, E. J. Ransley, D. Greaves, M. Hann, G. Iglesias, and B. Child, "Investigation of model validity for numerical survivability testing of wecs," 2017.

[16] E. Ransley, S. Yan, S. Brown, M. Hann, D. Graham, C. Windt, P. Schmitt, J. Davidson, J. Ringwood, P.-H. Musiedlak *et al.*, "A blind comparative study of focused wave interactions with floating structures (ccp-wsi blind test series 3)," *International Journal of Offshore and Polar Engineering*, vol. 30, no. 01, pp. 1–10, 2020.

[17] J. Westphalen, D. M. Greaves, A. Raby, Z. Z. Hu, D. M. Causon, C. G. Mingham, P. Omidvar, P. K. Stansby, B. D. Rogers *et al.*, "Investigation of wave-structure interaction using state of the art cfd techniques," *Open Journal of Fluid Dynamics*, vol. 4, no. 01, p. 18, 2014.

[18] L. Adegeest, "Use of nonlinear sea-load simulations in the design of ships," *Proceedings of PRADS'1998, Delft*, 1998.

[19] E. Quon, A. Platt, Y.-H. Yu, and M. Lawson, "Application of the most likely extreme response method for wave energy converters," in *ASME 2016 35th International Conference on Ocean, Offshore and Arctic Engineering*. American Society of Mechanical Engineers Digital Collection, 2016.

[20] B. J. Rosenberg, T. R. Mundon, R. G. Coe, E. W. Quon, C. C. Chartrand, Y.-H. Yu, and J. A. Van Rij, "Development of wec design loads: A comparison of numerical and experimental approaches," National Renewable Energy Lab.(NREL), Golden, CO (United States), Tech. Rep., 2019.

[21] R. G. Coe, B. J. Rosenberg, E. W. Quon, C. C. Chartrand, Y.-H. Yu, J. Van Rij, and T. R. Mundon, "Cfd design-load analysis of a two-body wave energy converter," *Journal of Ocean Engineering and Marine Energy*, vol. 5, no. 2, pp. 99–117, 2019.
[22] J. Van Rij, Y.-H. Yu, Y. Guo, and R. G. Coe, "A wave energy converter design load case study," *Journal of Marine Science and Engineering*, vol. 7, no. 8, p. 250, 2019.
[23] M. Göteman, J. Engström, M. Eriksson, M. Hann, E. Ransley, D. Greaves, M. Leijon *et al.*, "Wave loads on a point-absorbing wave energy device in extreme waves," in *The Twenty-fifth International Ocean and Polar Engineering Conference*. International Society of Offshore and Polar Engineers, 2015.
[24] M. Ochi, *Applied probability and stochastic processes*. New York: Wiley, 1990.
[25] S. Haver, K. Bruserud, G. S. Baarholm, and D. N. Veritas, "Environmental contour method: An approximate method for obtaining characteristic response extremes for design purposes," in *Proceedings of 13th International Workshop on Wave Hindcasting and Forecasting and 4th Coastal Hazard Symposium*, 2013.
[26] M. Christou and K. Ewans, "Field measurements of rogue water waves," *Journal of Physical Oceanography*, vol. 44, no. 9, pp. 2317–2335, 2014.
[27] D. N. Veritas, "Recommended practice dnv-rp-c205: environmental conditions and environmental loads," *DNV, Norway*, 2010.
[28] M. Drago, G. Giovanetti, and C. Pizzigalli, "Assessment of significant wave height–peak period distribution considering the wave steepness limit," in *International Conference on Offshore Mechanics and Arctic Engineering*, vol. 55393. American Society of Mechanical Engineers, 2013, p. V005T06A015.
[29] C. Schmittner, S. Kosleck, and J. Hennig, "A phase-amplitude iteration scheme for the optimization of deterministic wave sequences," in *International Conference on Offshore Mechanics and Arctic Engineering*, vol. 43468, 2009, pp. 653–660.
[30] J. Sutherland, A. Peet, and R. Soulsby, "Evaluating the performance of morphological models," *Coastal engineering*, vol. 51, no. 8-9, pp. 917–939, 2004.
[31] W.-T. Hsu, K. P. Thiagarajan, and L. Manuel, "Extreme mooring tensions due to snap loads on a floating offshore wind turbine system," *Marine Structures*, vol. 55, pp. 182–199, 2017.
[32] S. A. Sirigu, M. Bonfanti, E. Begovic, C. Bertorello, P. Dafnakis, G. Giorgi, G. Bracco, and G. Mattiazzo, "Experimental investigation of the mooring system of a wave energy converter in operating and extreme wave conditions," *Journal of Marine Science and Engineering*, vol. 8, no. 3, p. 180, 2020.